Supporting Information

Title Page

Exosome-encased Nucleic Acids Scaffold Chemotherapeutic Agents for Superior Anti-tumor and Anti-angiogenesis Activity

Author List

Ryan P. McNamara[1], Anthony B. Eason[1], Yijun Zhou[1], Rachele Bigi[1], Jack D. Griffith[1], Lindsey M. Costantini[1,2], Michelle A. Rudek[3], Nicole M. Anders[3], Blossom A. Damania[1], and Dirk P. Dittmer[1]*

Institution Addresses

[1]Lineberger Comprehensive Cancer Center and Department of Microbiology and Immunology, The University of North Carolina at Chapel Hill School of Medicine, 450 West Drive, Chapel Hill, NC, USA.

[2]Department of Biological and Biomedical Sciences, North Carolina Central University, 1801 Fayetteville St. Durham, NC, USA.

[3]Sidney Kimmel Comprehensive Cancer Center, Johns Hopkins School of Medicine, 401 N. Broadway, Baltimore, MD, USA

Table S1

Antibody	Manufacturer	Catalog Number	Use	Dilution
CD63	Santa Cruz Biotech	SC-15363	Immunoblot	1:500
CD81	Santa Cruz Biotech	SC-9158	Immunoblot	1:1,000
TSG101	Abcam	AB83	Immunoblot	1:1,000
DICER	Cell Signaling	3363	Immunoblot	1:1,000
β-actin	Cell Signaling	3700S	Immunoblot	1:10,000
CD9	Cell Signaling	13174	Immunoblot	1:1,000
Alix	Cell Signaling	92880S	Immunoblot	1:2,500
CD34	Novus	NB600-1071B	Immunofluorescence	1:200
Anti-mouse 680	Li-Cor	P/N925-32210	Immunoblot	1:10,000
Anti-rabbit 800	Li-Cor	P/N925-68071	Immunoblot	1:10,000
Anti-goat 680	Li-Cor	P/N925-68074	Immunoblot	1:10,000
LANA	Leica	13B10	Immunofluorescence	1:500
Phospho-γH2A.X	Cell Signaling	2577	Immunofluorescence	1:500
Anti-mouse AF350	Invitrogen	A1700384	Immunofluorescence	1:500
Anti-mouse Texas Red	Vector Bio	TI-2000	Immunofluorescence	1:500
Anti-rabbit AF 532	Invitrogen	A11009	Immunofluorescence	1:500
Anti-rabbit AF488	Thermo	A27034	Immunofluorescence	1:500
Anti-rat Fluorescein	Vector	FI-4000	Immunofluorescence	1:500

Table S1**.** List of antibodies, manufacturing origin, purpose, and dilutions used in this study.

Table S2

Phase	Variable	Value
Method Settings	Column Volume	0.962
Method Settings	Column	HiTrap CaptoCore 700 – 1 ml
Method Settings	High-Pressure Valve (MPa)	0.3
Method Settings	Flow Rate (ml/min)	0.5
Prime and Equilibration	Buffer A Wash Volume (ml)	5
Prime and Equilibration	PumpWash A Volume (ml)	5
Prime and Equilibration	Equilibration Volume (ml)	5
Sample Application	Last tube filled action	pause
Sample Application	Fraction Volume (ml)	0.5
Sample Application	Sample Volume (ml)	1
Sample Application	Chase Volume (ml)	0.5
Elution and Fractionation	Fixed Fractionation Volume (ml)	0.5
Elution and Fractionation	Elution Isocratic Volume (ml)	6

Table S2. List of settings used during total EV purification and fractionation on the AKTA Start.

Supplementary Figure Captions

Figure S1. Workflow for the isolation of EVs, incorporation of a drug, and affinity-purification of CD81+ EVs. Cross-flow filtration serves as an initial concentration and equilibration step, followed by polyethylene glycol (PEG) precipitation of the concentrated solution. The PEG precipitated EVs are then incubated with drug and nuclease to digest any non-encased nucleic acids. The solution is then passaged through high molecular weight chromatography to remove contaminants and non-incorporated drugs. Lastly, CD81+ EVs are affinity-purified using anti-CD81 beads and eluted for the final functional product.

Figure S2. Incorporation of doxorubicin of paclitaxel does not change EV size. The mean and mode sizes of purified EVs loaded with the indicated drug were quantified by nanoparticle tracking analysis (3 biological replicates with 11 technical replicates per experiment. Total events analyzed per technical replicate is >100 individual particles).

Figure S3. Primary tumor and plasma EVs can carry drugs. (A-D) Flow cytometry analysis of CD81+ KSHV-EVs taken from healthy donors (n = 5) on anti-CD81 beads, loaded with (A) DMSO, (B) DOX, (C) Paclitaxel Oregon Green 488, or (D) DOX and Paclitaxel. The horizontal axis shows fluorescence in the FITC channel, and the vertical axis shows fluorescence in the PE channel. (E) Size distribution analysis of eluted CD81+ EVs taken from healthy donors loaded with the indicated compound. Particle diameter is shown on the x-axis while occurrence is shown on the y-axis. A total of 11 technical replicates from 5 healthy donors is shown. (F) Mean and mode sizes of CD81+ EVs taken from healthy donors loaded with the indicated compound.

The vertical axis is the measured particle diameter (G-L) Same as A-F, but for CD81+ EVs taken from primary effusion lymphoma (PEL) fluid.

Figure S4. Loading of drugs or membrane intercalating dyes into CD81+ KSHV-EVs alters their mobility and zeta potential. KSHV-EVs, obtained from cultured PEL cells, were loaded with the indicated drug and affinity purified on anti CD81+ beads and eluted. Mobility and zeta potential was quantified through NTA with the charge at 25℃ at pH = 7.0 shown on the y-axis.

Figure S5**.** TEM image of CD81+ KSHV-EVs showing flexibility and malleability of the EV membrane. Scale bar is shown in lower left.

Figure S6**.** KSHV-derived miRNAs are readily detected in CD81+ KSHV-EVs. (A) Intracellular miRNAs from BCBL-1 cells were isolated and KSHV miRK12-10 was amplified using digital droplet reverse transcriptase PCR using KSHV-specific miRNA probes. (B) Dot plot representation of chip in A showing negative wells (yellow) and positive wells (blue). (C) RNase-treated AP CD81+ KSHV-EVs showing the presence of the KSHV miRK12-10 inside of EVs (protected from RNase). (D) Dot plot representation of chip in C showing negative wells and positive wells.

Figure S7**.** KSHV-EVs are adsorbed by endothelial cells in culture. (A-C) hTERT-HUVECs were treated with DMSO-CD81+ KSHV-EVs loaded with DMSO and stained for (A) Actin, (B) DiI, and (C) composite under 63x magnification. (D-F) Same as A-C, but with KSHV-HUVECs as recipient cells. (G-I) hTERT-HUVECs were treated with DiI-KSHV-EVs from PEL and

stained for (G) Actin, (H) DiI, and (I) composite. (J-L) Same as G-I, but for KSHV-HUVECs as recipient cells. (M-O) 100X magnification of hTERT-HUVECs treated with DiI-KSHV-EVs and stained for (M) Actin, (N) DiI, and (O) composite. (P-R) Same as M-O, but with KSHV-HUVECs as recipient cells.

Figure S8**.** Doxorubicin delivered by KSHV-EVs induces DNA damage in EC. (A-D) hTERT-HUVECs were seeded and mock-treated for 24 hours and then stained for (A) DAPI, (B) Actin, (C) phospho-γH2A.X, and (D) composite. (E-H) hTERT-HUVECs were treated with DMSO-CD81+ KSHV-EVs cells for 24 hours and then stained for (E) DAPI, (F) Actin, (G) phospho-γH2A.X, and (H) composite. (I-L) Same as E-H, but for hTERT-HUVECs treated with Doxo-CD81+ EVs. (M-P) hTERT-HUVECs were treated with the liposomal formulation of doxorubicin, Doxil, for 24 hours and then stained for (M) DAPI, (N) Actin, (O) phospho-γH2A.X, and (P) composite. (Q-T) Same as M-P, but for the drug doxorubicin alone. (U) Quantification of the number of cells showing DNA damage as judged by staining of phospho-γH2A.X. Positive phospho-γH2A.X cells was divided by the total number of nuclei in a field of view in a total of five separate fields of view.

Figure S9. Paclitaxel delivered by KSHV-EVs stalls EC division. (A-D) hTERT-HUVECs were seeded and treated with DMSO -CD81+ KSHV-EVs for 24 hours and then stained for (A) Actin, (B) Paclitaxel Oregon Green 488, and (C) composite. (D-F) Same as A-C, but for KSHV-HUVECs as recipient cells. (G-I) hTERT-HUVECs were seeded and treated with Paclitaxel KSHV-EVs for 24 hours and then stained for (G) Actin, (H) Paclitaxel Oregon Green 488, and (I) composite. (J-L) Same as G-I, but for KSHV-HUVECs. (M-O) 100X objective magnification

of hTERT-HUVECs treated with Paclitaxel KSHV-EVs for 24 hours and then stained for (M) Actin, (N) Paclitaxel Oregon Green 488, and (O) composite. (P-R) Same as M-O, but for KSHV-HUVECs.

Figure S10. Drug-loaded KSHV-EV can be safely administered *in vivo*. Mice were subcutaneously administered Matrigel loaded with (A) PBS, (B) VEGF, (C) Dil-KSHV-EV, and (D) DOX-KSHV-EV. After 7 days, mice were sacrificed and the sites of the Matrigel plug were removed and assayed for overall histology prior to thin sectioning microscopy. Shown are representative images of plugs removed from mice at the end of the experiment. No differences were observed between male and female cohorts. The isolated tissue was fixed in formalin prior to thin sectioning.

Figure S11**.** Endothelial cells are recruited to the site of delivered KSHV-EVs and uptake the labeled EVs. (A-D) The negative control of PBS/saline Matrigel port was removed from mouse post sacrifice and stained with (A) DAPI, (B) CD34, (C) DiI Channel, and (D) Composite. (E-H) Same as A-D, but for VEGF Matrigel. (I-L) CD81+ KSHV-EVs were labeled with the membrane dye DiI and administered subcutaneously through Matrigel. (M-P) Same as I-L, but for KSHV-EVs loaded with DOX (DOX-KSHV-EVs). Scale bar = 40 μm. All images were taken 7 days after injection.

Figure S12. KSHV-EVs deliver functional drugs to target cells *in vivo*. (A) PBS/saline Matrigel port was removed from mouse post sacrifice and stained with DAPI (cyan), DiI (magenta), and the DNA damage marker phospho-γH2A.X (yellow). (B) Same as A, but for mice treated with

VEGF. (C) Same as A, but for mice treated with DiI-KSHV-EVs. (D) Same as A, but for mice treated with DOX-KSHV-EVs. (E-H) Grayscale images of A-D for phospho-γH2A.X. Non-nuclear staining of phospho-γH2A.X represents apoptotic debris as mice were treated with DOX-KSHV-EVs for 7 days before tissue excision – in contrast with tissue culture condition of 24 hours. Scale bar = 40 μm.

Figure S13**.** DICER KO cells do not contain miRNAs inside of EVs. CD81+ EVs from WT and DICER KO cells were obtained and nucleic acids were purified. miRNAseq of the nucleic acid fraction of the EVs was done. As a quality control measure, a spike-in control for the DICER KO nucleic acid preparation was added during the column purification stage.

Figure S14. Total EV production and biophysical characteristics of EVs are not altered by DICER KO. (A) Size distribution analysis of EVs obtained from the supernatant of WT and DICER KO 293T cells as determined by NTA. EV diameter is shown on the x-axis and relative occurrence is shown on the y-axis for WT and DICER KO cell lines. (B) The concentration of EVs from the supernatant of WT and DICER KO 293T cells. (C) The mean and mode sizes of EVs were obtained from the supernatant of WT and DICER KO 293T cells. EV diameter is shown on the y-axis. For all experiments, 11 technical replicates from 3 independent biological replicates are shown.

Figure S15. EVs with miRNAs incorporate and retain higher concentrations of Paclitaxel. (A) MFI of EVs immobilized on anti-CD81 beads from WT or DICER KO 293T cells loaded with

DMSO or Paclitaxel-Oregon Green 488. (B) Same as A, but for EVs loaded with the membrane dye DiI and analyzed on the PE channel.

Figure S16. Transfer of doxorubicin from Doxil to EVs does not alter EV size. EVs containing CD63-GFP were incubated with Doxil to transfer the incorporated drug over time. EVs were affinity purified on CD81 beads, eluted, and assayed for mean and mode sizes. No trend in size changes in the EVs was identified, arguing against membrane fusion or incorporation of Doxil inside of an EV (n = 3 with 11 technical replicate measurements). On the right is the heatmap scale bar.

Supplementary Figure 1

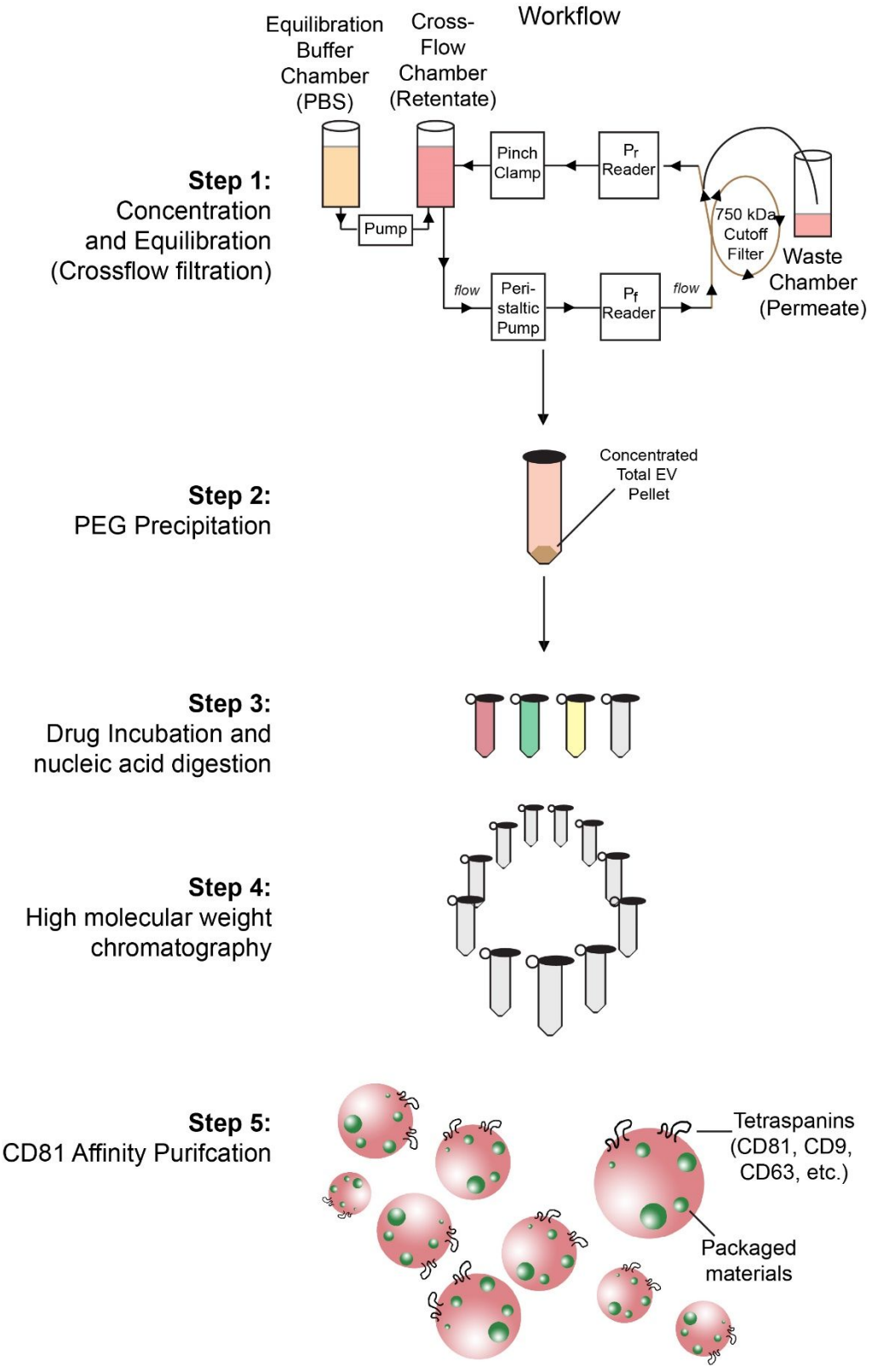

Supplementary Figure 2

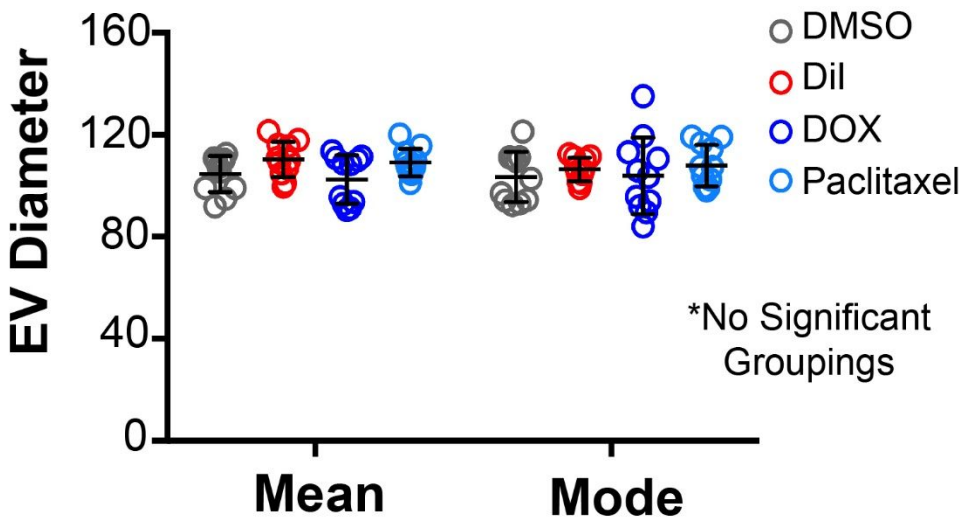

Supplementary Figure 3

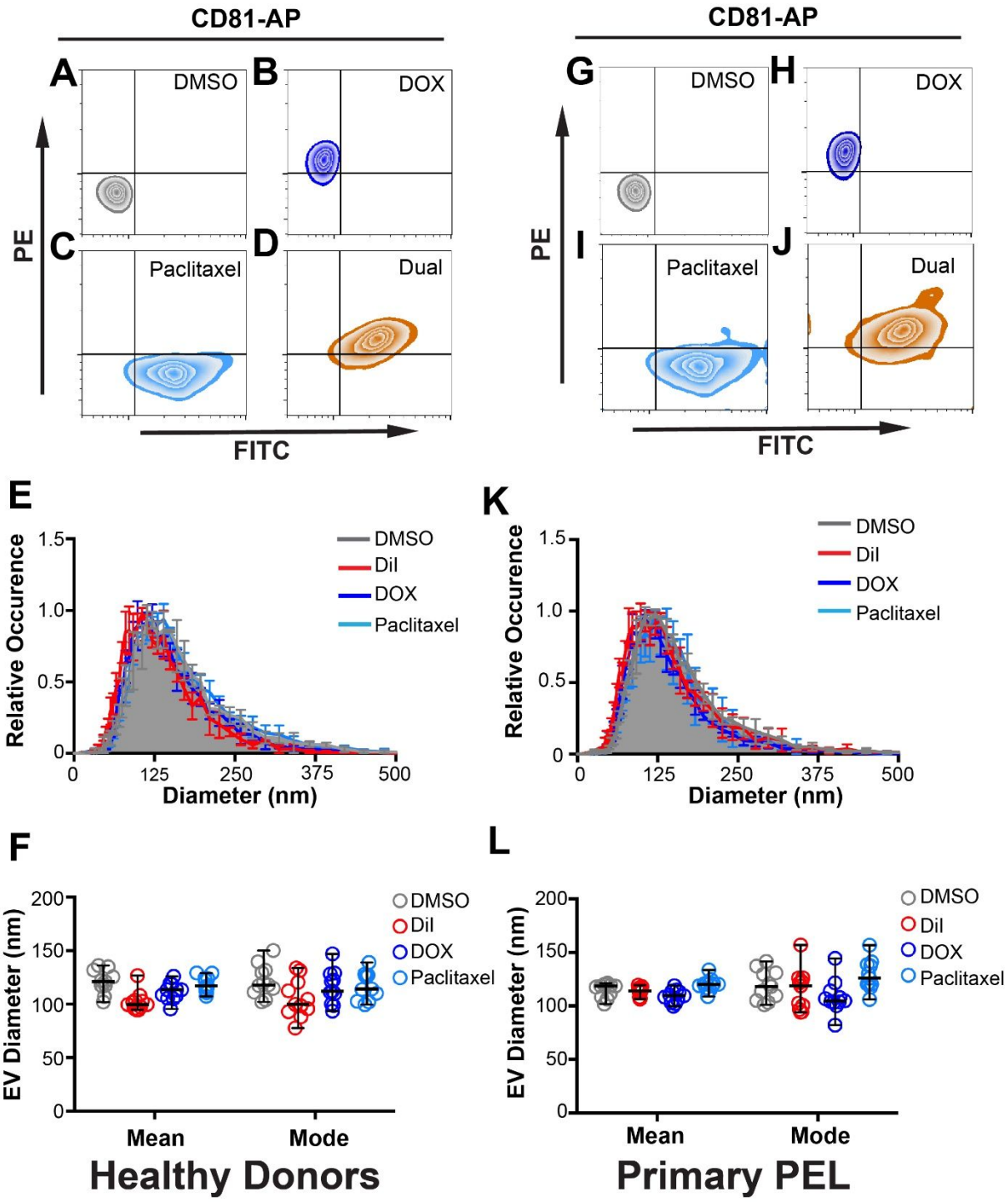

Supplementary Figure 4

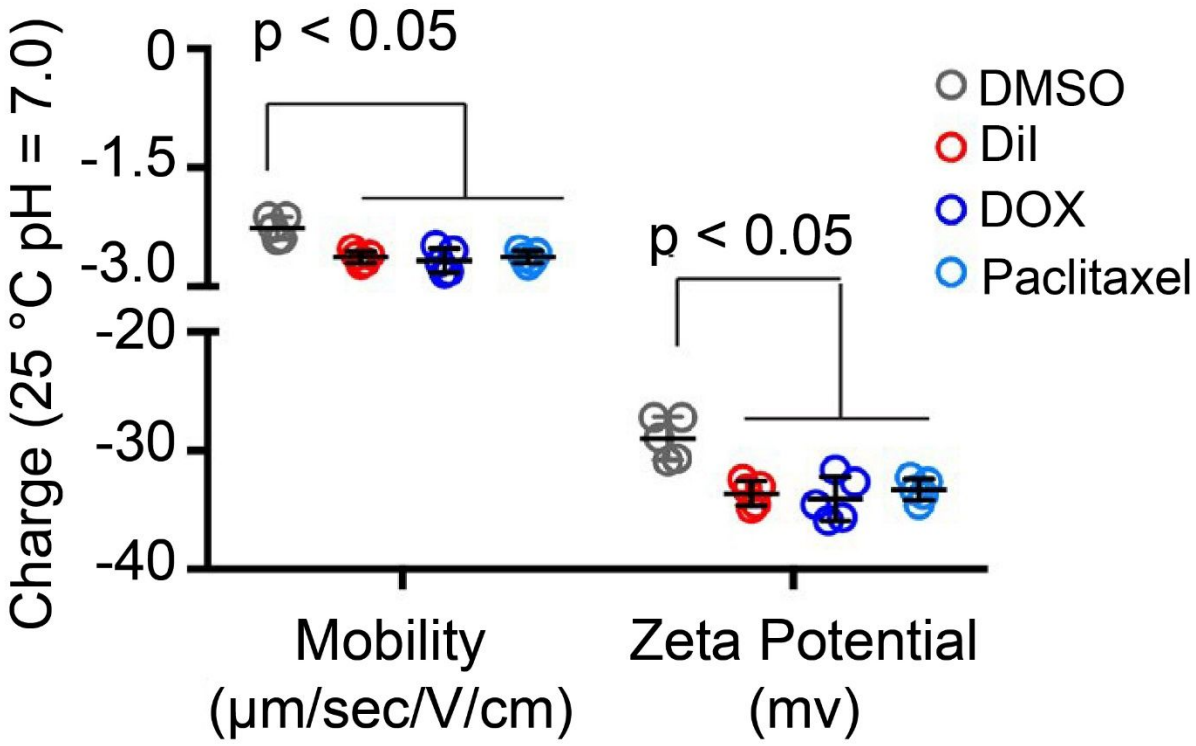

Supplementary Figure 5

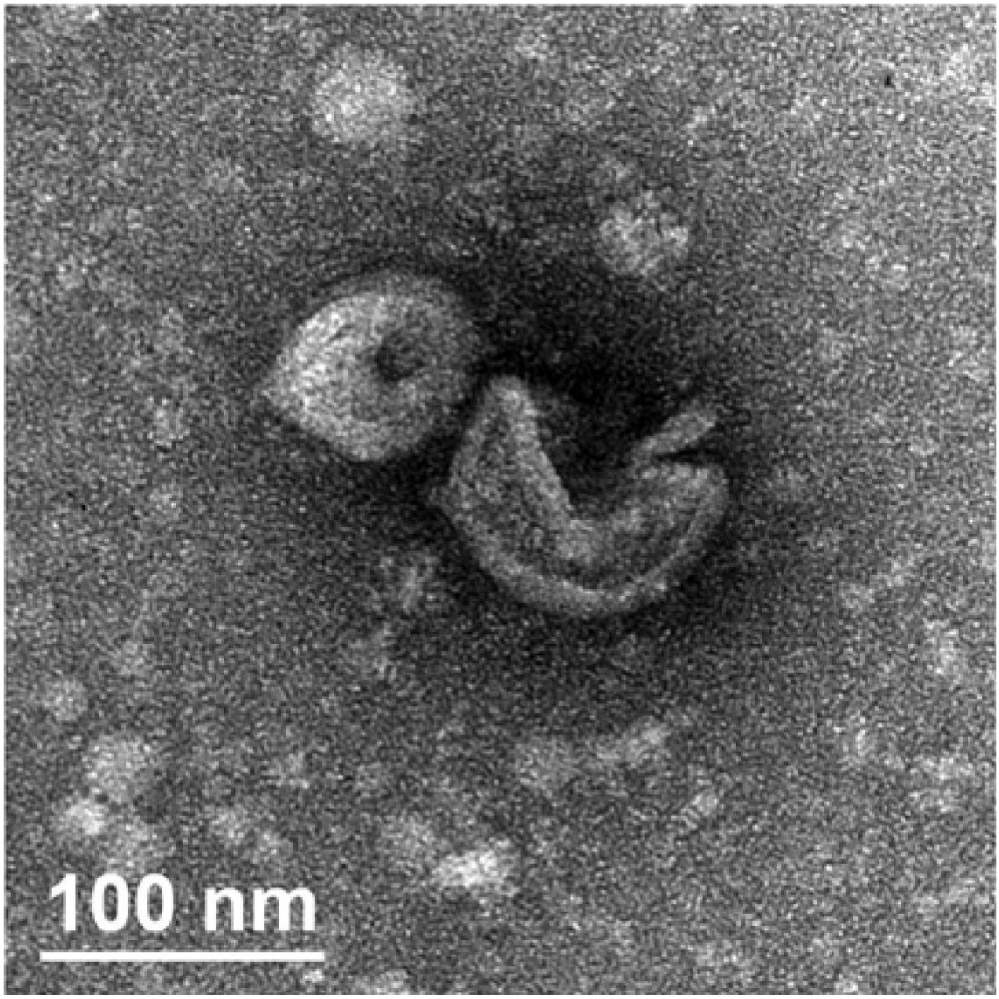

Supplementary Figure 6

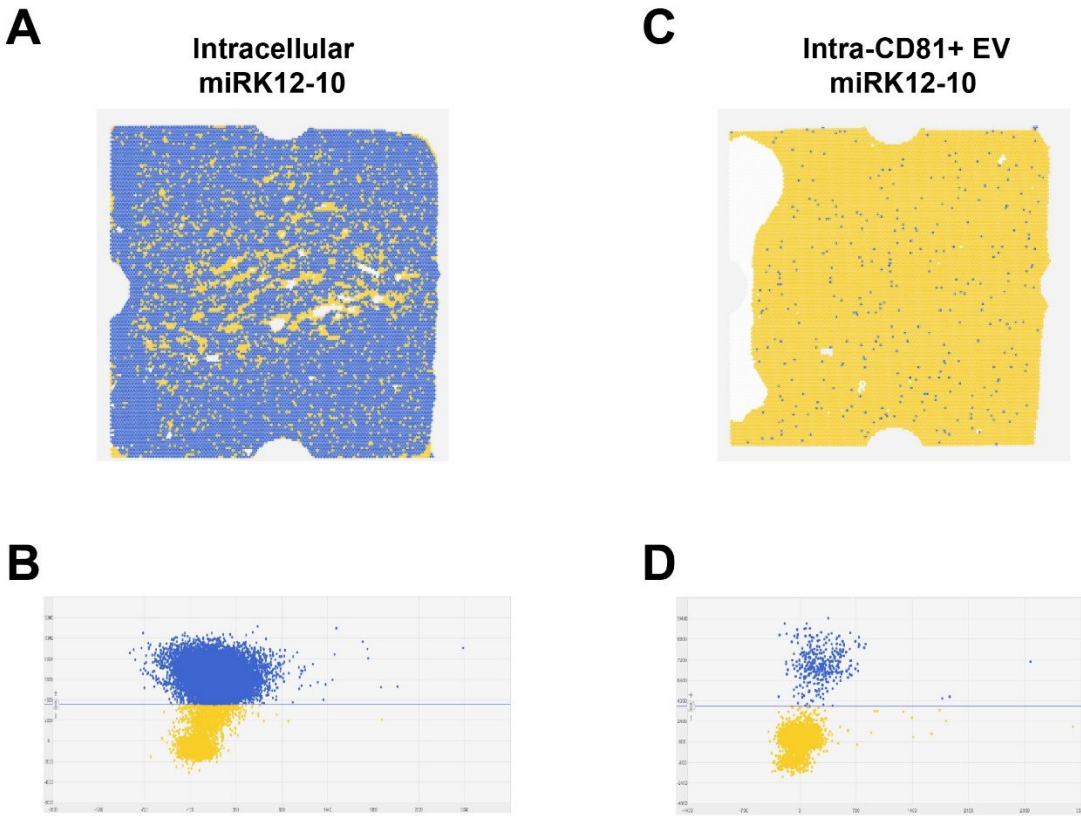

Supplementary Figure 7

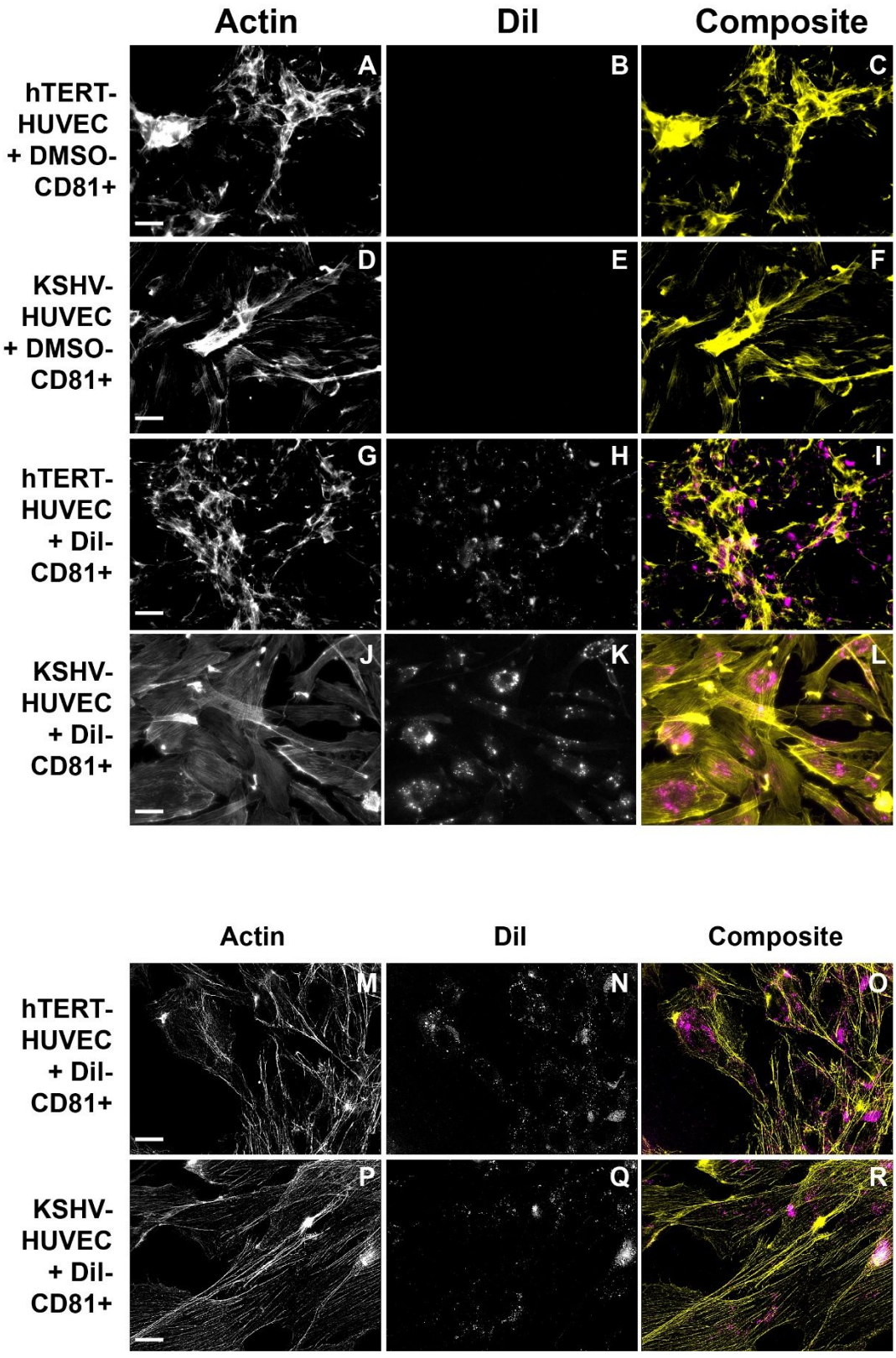

Supplementary Figure 8

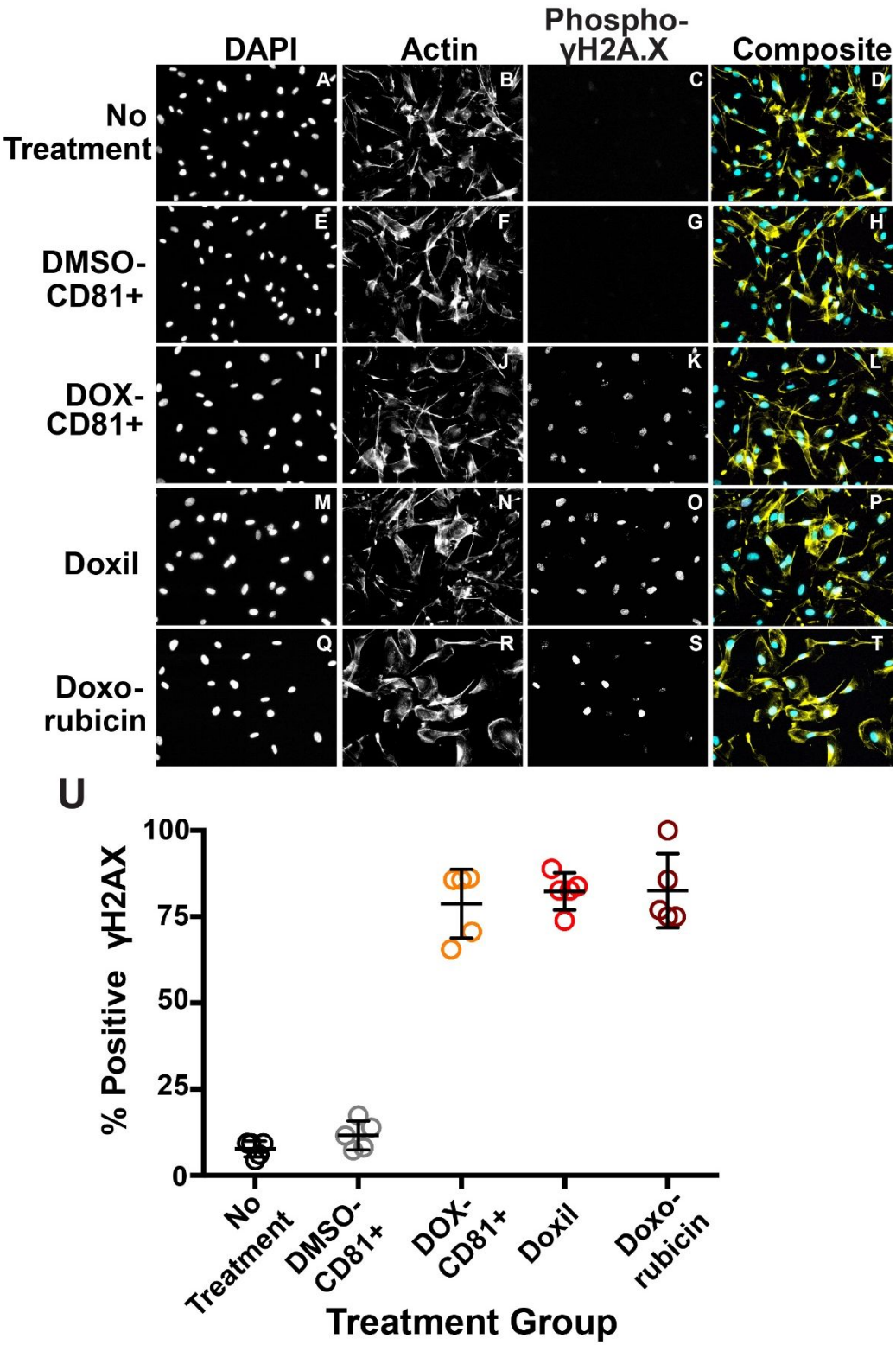

Supplementary Figure 9

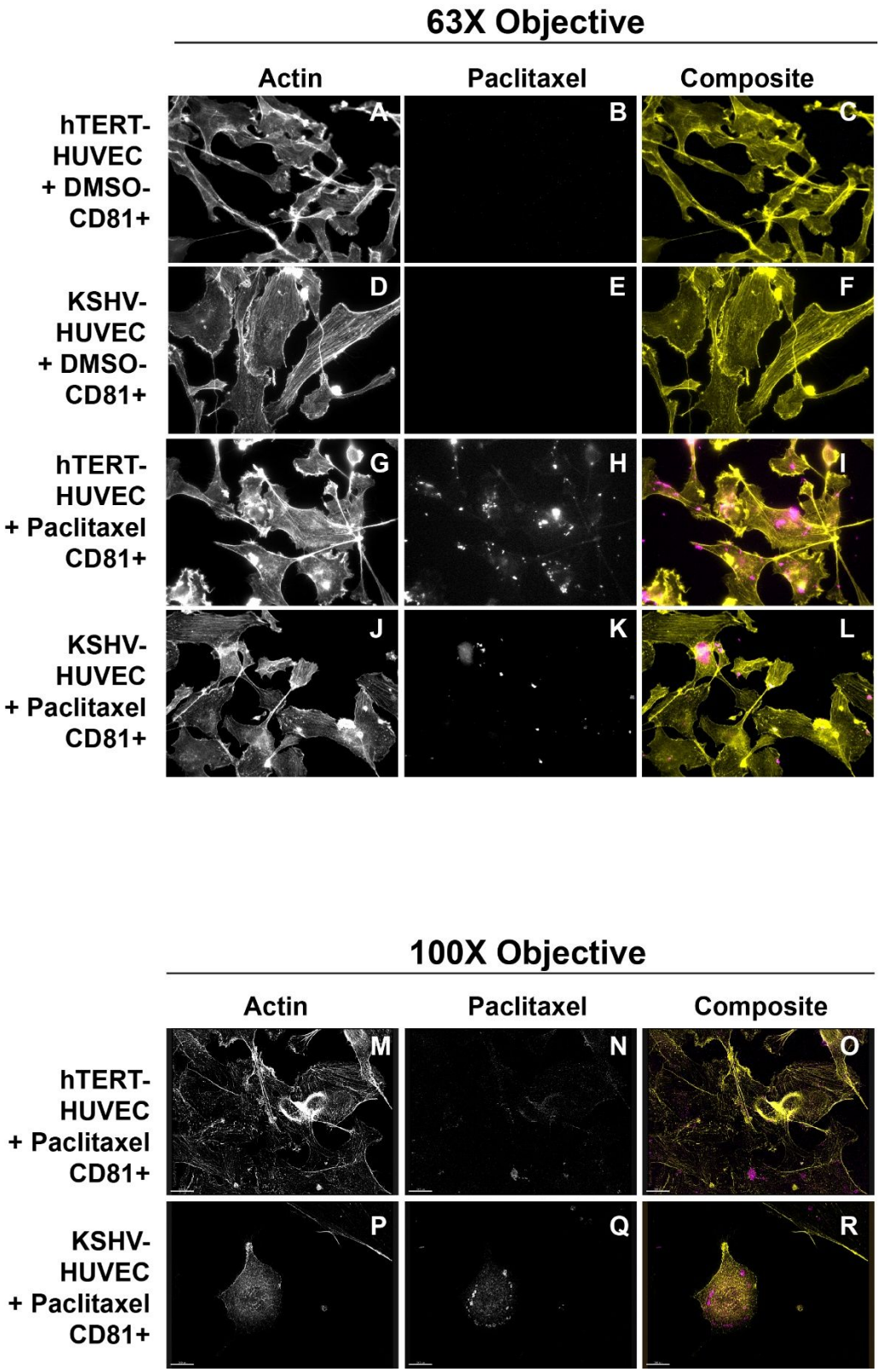

Supplementary Figure 10

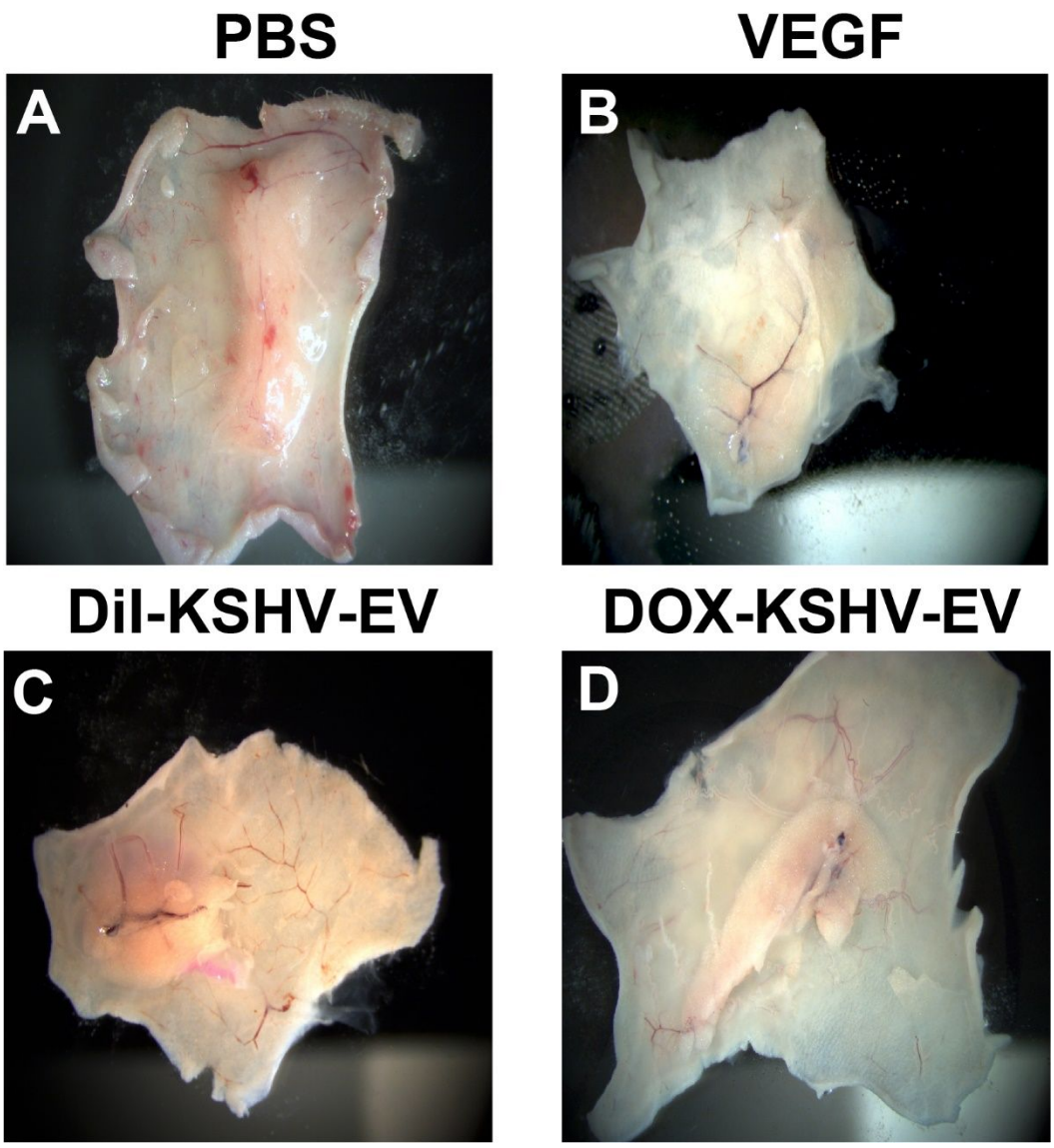

Supplementary Figure 11

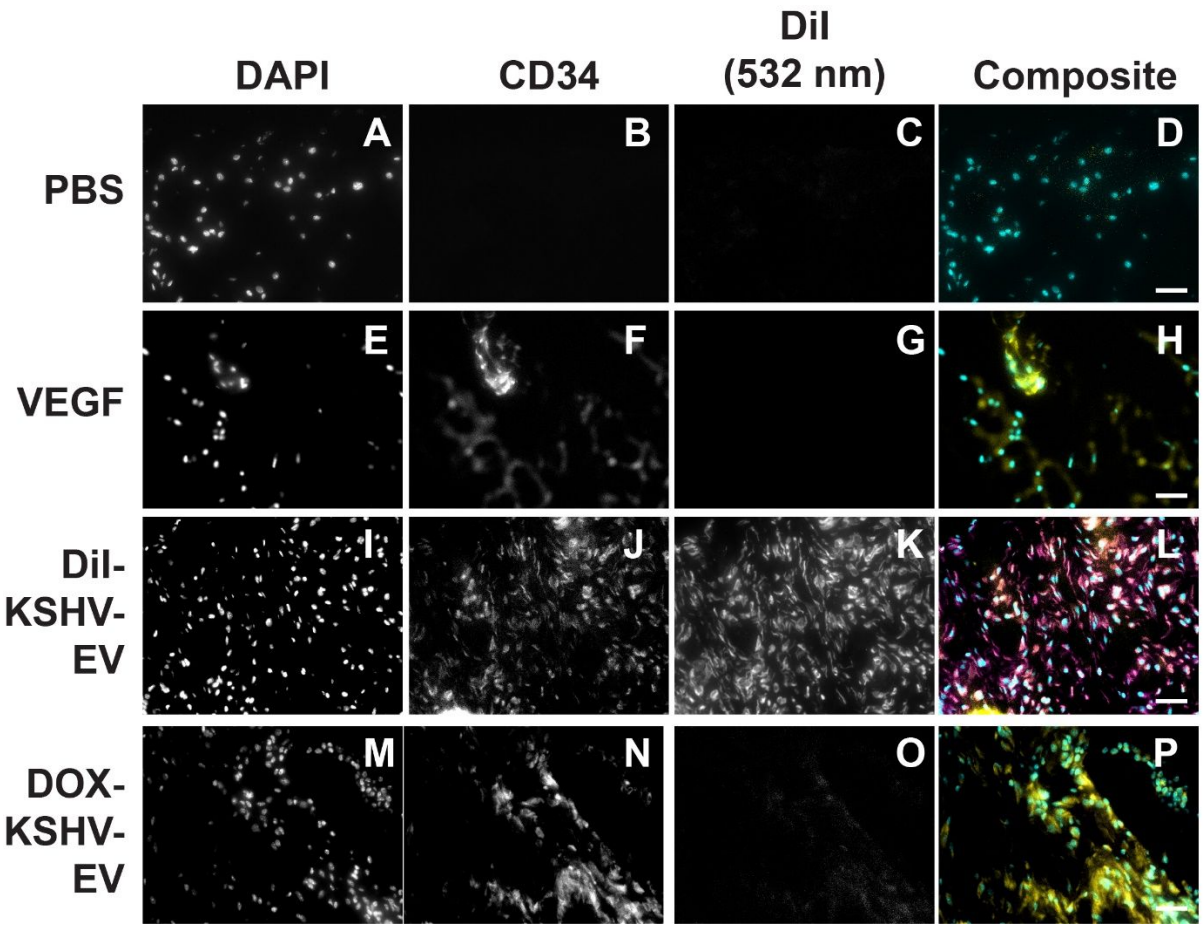

Supplementary Figure 12

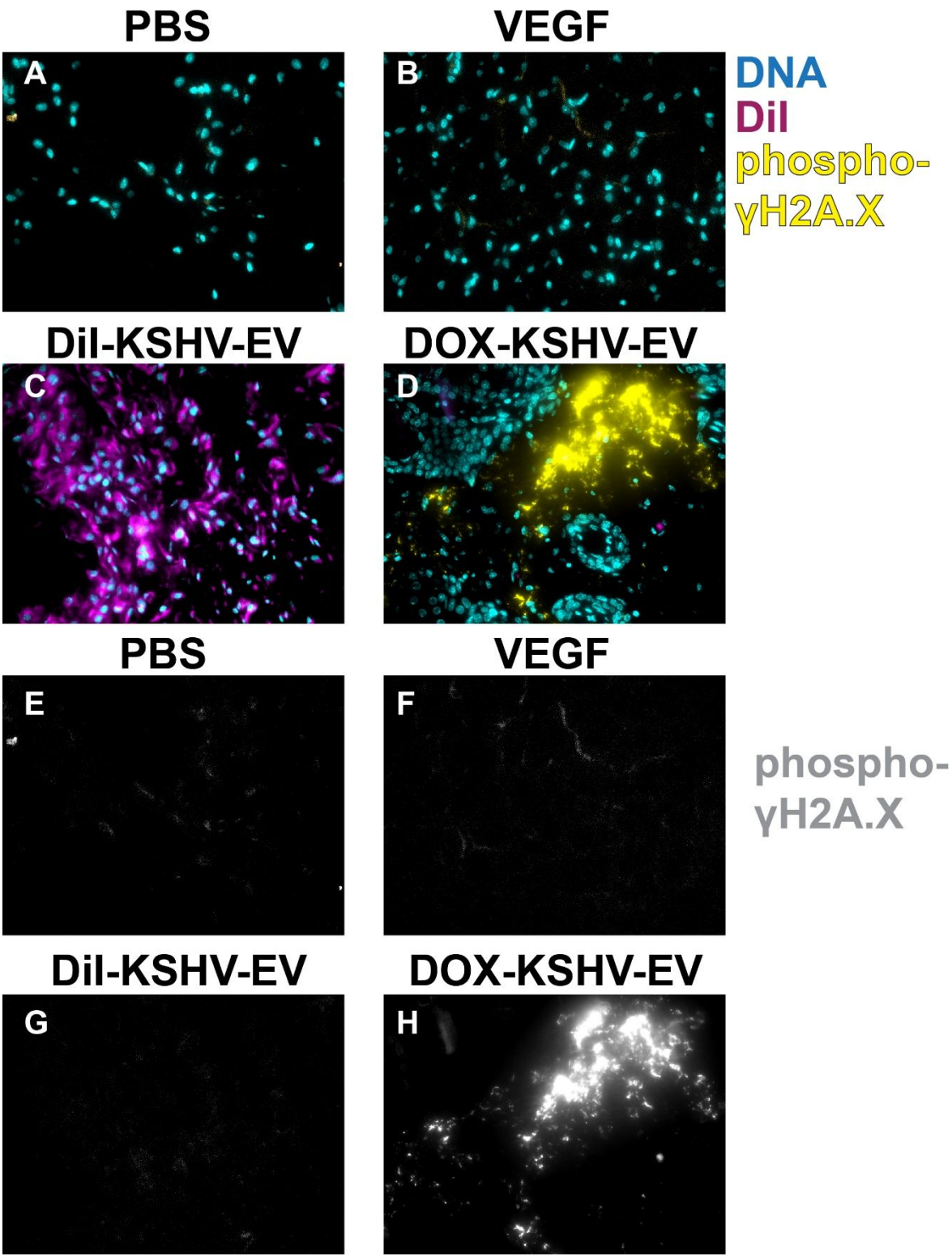

Supplementary Figure 13

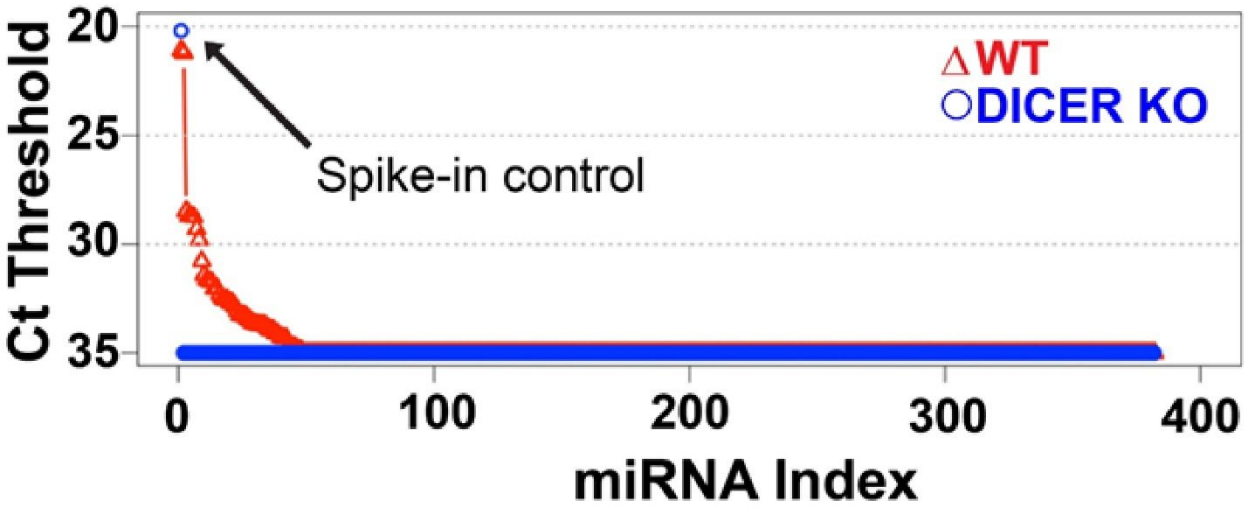

Supplementary Figure 14

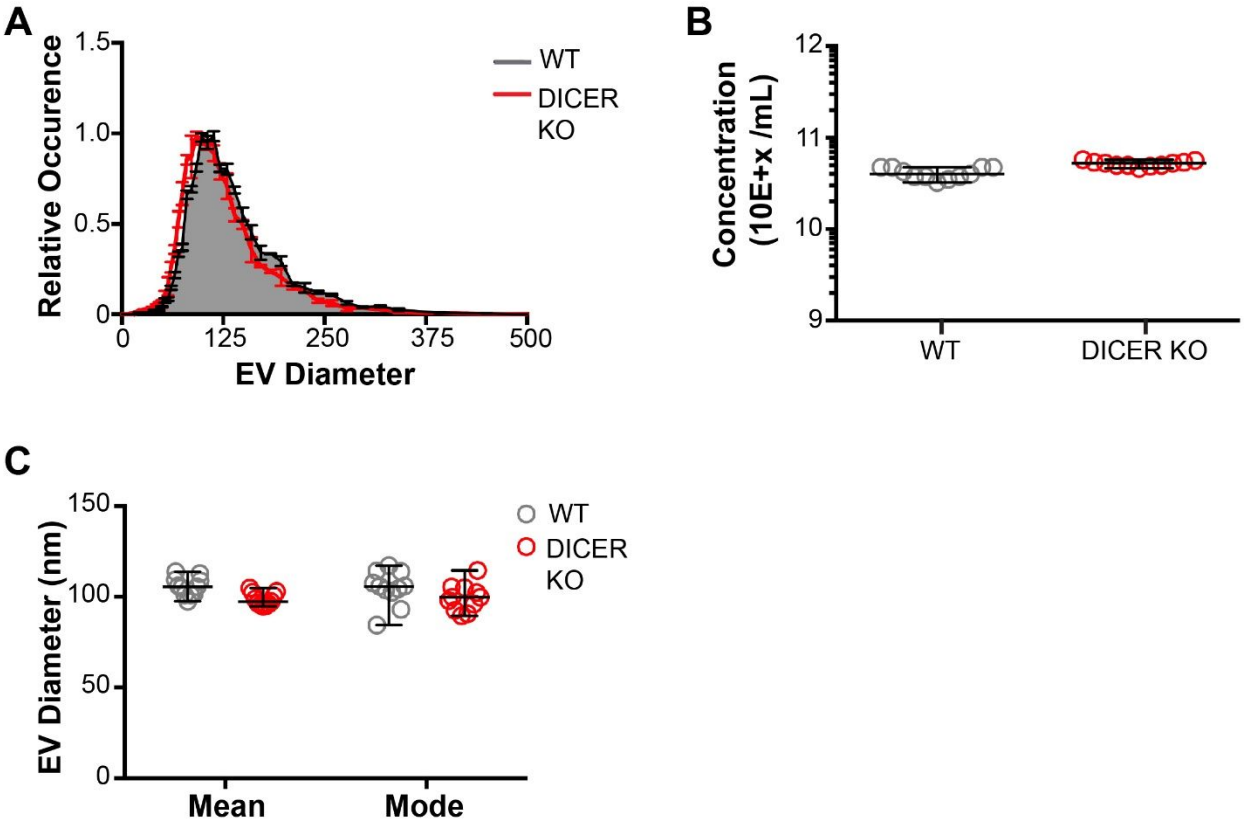

Supplementary Figure 15

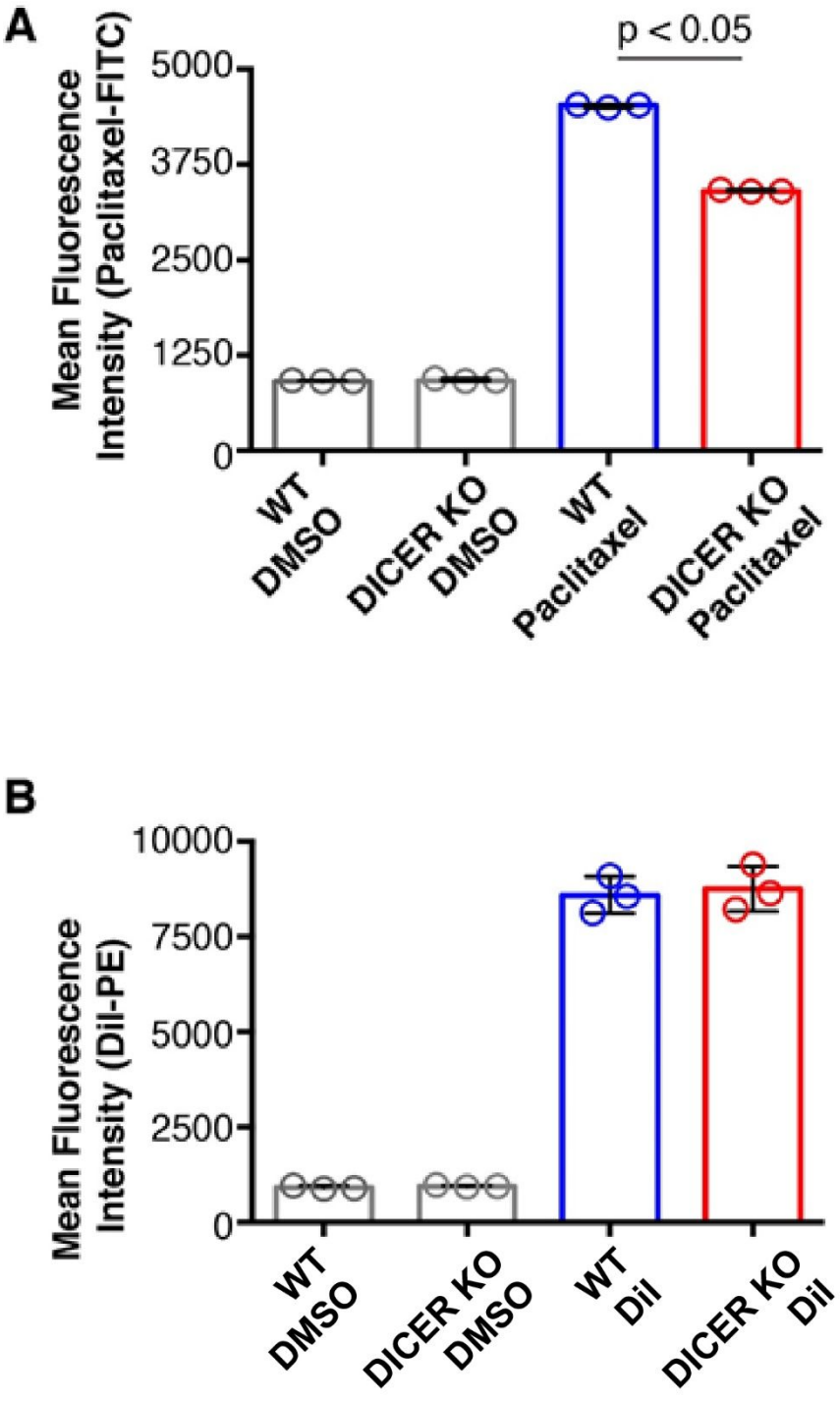

Supplementary Figure 16